CrossMark

J. Fluid Mech. (2018), *vol.* 855, *pp.* 181–209. © Cambridge University Press 2018
doi:10.1017/jfm.2018.626

Marangoni-enhanced capillary wetting in surfactant-driven superspreading

Hsien-Hung Wei†

Department of Chemical Engineering, National Cheng Kung University, Tainan 701, Taiwan

(Received 14 November 2017; revised 1 April 2018; accepted 31 July 2018;
first published online 14 September 2018)

Superspreading is a phenomenon such that a drop of a certain class of surfactant on a substrate can spread with a radius that grows linearly with time much faster than the usual capillary wetting. Its origin, in spite of many efforts, is still not fully understood. Previous modelling and simulation studies (Karapetsas *et al. J. Fluid Mech.*, vol. 670, 2011, pp. 5–37; Theodorakis *et al. Langmuir*, vol. 31, 2015, pp. 2304–2309) suggest that the transfer of the interfacial surfactant molecules onto the substrate in the vicinity of the contact line plays a crucial role in superspreading. Here, we construct a detailed theory to elaborate on this idea, showing that a rational account for superspreading can be made using a purely hydrodynamic approach without involving a specific surfactant structure or sorption kinetics. Using this theory it can be shown analytically, for both insoluble and soluble surfactants, that the curious linear spreading law can be derived from a new dynamic contact line structure due to a tiny surfactant leakage from the air–liquid interface to the substrate. Such a leak not only establishes a concentrated Marangoni shearing toward the contact line at a rate much faster than the usual viscous stress singularity, but also results in a microscopic surfactant-devoid zone in the vicinity of the contact line. The strong Marangoni shearing then turns into a local capillary force in the zone, making the contact line in effect advance in a surfactant-free manner. This local Marangoni-driven capillary wetting in turn renders a constant wetting speed governed by the de Gennes–Cox–Voinov law and hence the linear spreading law. We also determine the range of surfactant concentration within which superspreading can be sustained by local surfactant leakage without being mitigated by the contact line sweeping, explaining why only limited classes of surfactants can serve as superspreaders. We further show that spreading of surfactant spreaders can exhibit either the $1/6$ or $1/2$ power law, depending on the ability of interfacial surfactant to transfer/leak to the bulk/substrate. All these findings can account for a variety of results seen in experiments (Rafai *et al. Langmuir*, vol. 18, 2002, pp. 10486–10488; Nikolov & Wasan, *Adv. Colloid Interface Sci.*, vol. 222, 2015, pp. 517–529) and simulations (Karapetsas *et al.* 2011). Analogy to thermocapillary spreading is also made, reverberating the ubiquitous role of the Marangoni effect in enhancing dynamic wetting driven by non-uniform surface tension.

Key words: contact lines, interfacial flows (free surface), lubrication theory

† Email address for correspondence: hhwei@mail.ncku.edu.tw

https://doi.org/10.1017/jfm.2018.626 Published online by Cambridge University Press

1. Introduction

When a drop of a solution of a certain class of surfactants such as trisiloxane is placed on a solid substrate, it can spread at an unusually fast rate much higher than a surfactant-free solution (Hill 1988; Zhu *et al.* 1994; Stoebe *et al.* 1996). Rafai *et al.* (2002) reported that this so-called superspreading can occur at a strikingly fast rate with the spreading radius growing linearly with time, $R \propto t$ – the power is 10 times greater than that of Tanner's law (Tanner 1979). Although there are extensive studies (Beacham, Matar & Craster 2009; Karapetsas, Craster & Matar 2011; Wang *et al.* 2013; Theodorakis *et al.* 2015) and related investigations (Joanny 1989; Jensen & Grotberg 1992; Clay & Miksis 2004; Jensen & Naire 2006), the true nature of superspreading is still not fully understood. It is generally believed that the Marangoni force caused by the surface tension gradient $\boldsymbol{\nabla}_s\sigma$ plays a major role in superspreading phenomenon (Rafai *et al.* 2002; Nikolov & Wasan 2015). This force can drive a fluid at velocity

$$u_M = h\boldsymbol{\nabla}_s\sigma/\eta, \tag{1.1}$$

where h is the drop height and η the viscosity of the wetting fluid. However, the spreading exponent is often found to be far below unity (Jensen & Grotberg 1992; Starov, de Ryck & Velarde 1997; Jensen & Naire 2006). In fact, it is impossible to derive the linear spreading law by having $\boldsymbol{\nabla}_s\sigma$ across the drop spreading radius R, especially when additional global constraints (i.e. constant drop volume and surfactant mass conservation) are imposed. This implies that the Marangoni force alone does not suffice to account for this unusual spreading caused by surfactant superspreaders. Other effects might involve surfactant assembly (Stoebe *et al.* 1997; Kumar *et al.* 2003*a*), surfactant adsorption on the solid surface (Kumar, Couzis & Maldarelli 2003*b*) and surfactant transport at the contact line (Clay & Miksis 2004). Karapetsas *et al.* (2011) developed a lubrication model by including all the above effects and showed that the linear spreading law can be captured due to delicate interplays between these effects. In particular, whether interfacial surfactant molecules can be transferred onto the solid substrate in the vicinity of the contact line seems to play a crucial role in superspreading (Kim, Qin & Fichthorn 2006; Karapetsas *et al.* 2011; Maldarelli 2011; Theodorakis *et al.* 2015).

In fact, because $u_M \propto h\ \boldsymbol{\nabla}_s\sigma$ according to (1.1), to attain a constant spreading speed and hence the linear spreading law, $\boldsymbol{\nabla}_s\sigma$ in (1.1) needs to be established over the drop height h (Rafai *et al.* 2002; Rafai & Bonn 2005). If the above is true, because u_M is invariant with h, h in (1.1) can be taken as any local thickness of a drop that varies roughly linearly with the distance to the contact line. Taking $h \to 0$, the contact line (which is moving at speed U) would have to be driven by a local Marangoni shearing $\boldsymbol{\nabla}_s\sigma \propto 1/h$ that diverges as fast as the usual moving contact line stress singularity $\eta U/h$ (Huh & Scriven 1971). This might explain why the spreading speed is independent of the extent of spreading. This also implies that a rational explanation of the linear spreading law can only be sought by resolving what happens near the moving contact line.

Therefore, to obtain the linear spreading law, it is necessary to examine how both the flow field and surfactant transport behave in the vicinity of the contact line during a superspreading process. It is worth mentioning that in the simulation study by Karapetsas *et al.* (2011), the relationship between the dynamic contact angle and wetting spread is assumed to obey the clean-interface de Gennes–Tanner cubic law. However, it is not obvious that this has to be the case. In fact, existing theoretical studies showed that modified wetting relationships can result from a Marangoni stress

https://doi.org/10.1017/jfm.2018.626 Published online by Cambridge University Press

induced by surfactant (Cox 1986*b*; Joanny 1989; Chesters & Elyousfi 1998; Rame 2001; Chan & Borhan 2006; Jensen & Naire 2006). So the successful capture of the linear spreading law by Karapetsas *et al.* (2011) seems to imply that the classical de Gennes–Tanner law might be the correct wetting law for surfactant superspreaders, but not for regular surfactants whose spreading powers are smaller than unity. If this is the case, a completely different contact line structure must exist for the former to accommodate the de Gennes–Tanner law when a Marangoni stress is present. The resolution of this contact line structure will not only complement the simulation study by Karapetsas *et al.* (2011), but also provide more insights into how the linear spreading law results from the transport of superspreaders.

Motivated by the above, we aim at developing a dynamic contact line theory for surfactant-driven superspreading. How to construct such a theory by acquiring key ingredients of superspreading is described as follows. As mentioned earlier, the key to obtaining the linear spreading law lies in a concentrated Marangoni stress in the vicinity of the contact line. As such a Marangoni stress has to act toward the contact line, the interfacial surfactant concentration near the contact line has to be much lower than that away from the contact line. From a mass transfer point of view, a 'sink' or some sort of depletion mechanism must exist to draw surfactant molecules out of the air–liquid interface to sustain this local surfactant deficiency near the contact line. It has also been shown previously that the adsorption of surfactant molecules onto the substrate from the interface is one of key elements to superspreading (Karapetsas *et al.* 2011; Theodorakis *et al.* 2015). Therefore, in order to take account of such surfactant depletion or adsorption effects in a simpler way, in this work we prescribe a local surfactant leakage flux in the vicinity of the contact line in the surfactant transport equation. This will directly set-up an interfacial surfactant concentration gradient to drive the contact line with Marangoni stress. As illustrated in figure 1, such leakage can occur in two different routes, depending on whether surfactant molecules on the interface can undergo mass exchange with the bulk. For insoluble surfactant, because it cannot be desorbed back to the bulk, its leakage can only occur along the interface via its direct transfer through the contact line (see figure 1*a*). In contrast, for soluble surfactant, its leakage can be through the bulk, achieved by corner diffusion from the interface to the substrate inside the drop (see figure 1*b*).

The above routes to the depletion of interfacial surfactant have been suggested in the modelling and simulation studies by Karapetsas *et al.* (2011) and Theodorakis *et al.* (2015). In their studies, the interfacial surfactant concentration gradient needed for promoting drop spreading is established by delicate interplays between surfactant molecules on the interface and those in the bulk and on the substrate. In contrast, in this work we stipulate the surfactant depletion near the contact line as the sole driving mechanism for superspreading and model it as a local surfactant leakage flux. As will be demonstrated, by incorporating this local surfactant leakage explicitly into the contact line hydrodynamics, we can theoretically show that superspreading is in effect a new class of dynamic wetting: *Marangoni-enhanced capillary wetting* – the joint wetting mechanism unique to superspreaders by having both surface tension and surface tension gradient forces work collaboratively.

This Marangoni–capillary wetting will not only call for a new contact line structure, but also provide a natural explanation for the linear spreading law. As will also be shown by this work, it is actually a direct consequence of the features below arising from local surfactant leakage. First, a fraction of surfactant leakage can set-up a concentrated Marangoni shearing toward the contact line with a Marangoni stress singularity diverging at a rate much faster than the usual viscous stress singularity.

https://doi.org/10.1017/jfm.2018.626 Published online by Cambridge University Press

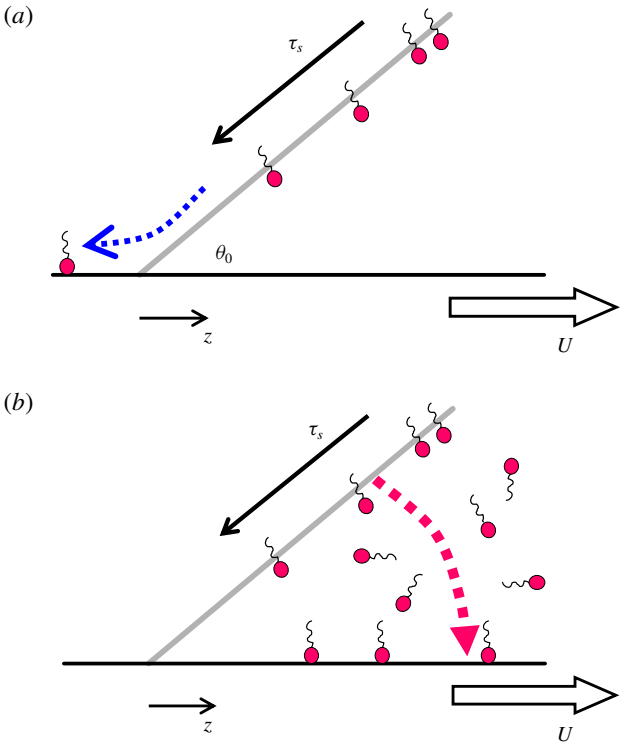


FIGURE 1. (Colour online) Schematic illustration of surfactant-enhanced spreading. A Marangoni force toward the contact line can be established by an interfacial surfactant concentration gradient set-up by a local surfactant leakage. Such leakage can occur via two different routes, depending on whether surfactant molecules on the interface can undergo mass exchange with the bulk. (*a*) For insoluble surfactant, its leak can only occur along the interface via its direct transfer through the contact line. (*b*) For soluble surfactant, its leakage can be achieved through corner diffusion from the interface to the substrate inside the drop.

Second, this leak also results in a microscopic surfactant-devoid zone in the vicinity of the contact line. Because the contact line is free of surfactant, the strong Marangoni shearing does not drive the contact line directly but turns into a local capillary force, driving the contact line to advance in a purely capillary manner. Third, as a result of this local Marangoni-driven capillary wetting, the contact line is moving at a constant wetting speed governed by the de Gennes–Tanner law, thereby leading to the linear spreading law. Finally, we also determine the range of the leakage flux within which superspreading can occur without being mitigated by the contact line sweeping. This explains why superspreading occurs in a range of surfactant concentration and why only limited classes of surfactants can serve as superspreaders.

The rest of the paper derives the above results according to the following outline. In § 2 we begin with the lubrication formulation to provide the basic equations needed for modelling superspreading. Using this formulation, we first consider insoluble surfactant in § 3 and demonstrate a possible realization of superspreading. This will elicit key features of superspreading. Detailed accounts for soluble surfactant will be given in § 4, which is more relevant to superspreading. In § 5 we make connections

https://doi.org/10.1017/jfm.2018.626 Published online by Cambridge University Press

of our findings to a variety of results seen in experiments and simulations. A criterion of superspreading will also be established. In § 6 we show that an analogy can exist between surfactant-driven spreading and thermocapillary spreading, highlighting the exclusive role of the Marangoni effect in dynamic wetting driven by non-uniform surface tension. The paper is finally concluded in § 7.

2. Formulation and basic equations

Similar to the analysis by Joanny (1989), we assume that the region near the contact line is approximately wedge shaped with the macroscopic contact angle θ_0. We further assume that θ_0 is sufficiently small so that the liquid height can be approximated as $h = \theta_0 x$. This small angle assumption allows us to apply the lubrication theory to derive the relevant equations. In the frame moving with the contact line speed U, the horizontal velocity u satisfies the lubrication equation $p_x = \eta u_{yy}$ with boundary conditions $u = U$ at $y = 0$ and $\eta u_y = \tau_s$ at $y = h$. The solution is then given by

$$u = (p_x/2\eta)[y^2 - 2hy] + \tau_s y/\eta + U. \tag{2.1}$$

Here the Marangoni stress τ_s is written as the interfacial surfactant concentration gradient Γ_x according to

$$\tau_s = -\beta \Gamma_x, \tag{2.2}$$

where $\beta \equiv -(\partial\sigma/\partial\Gamma)$ measures the susceptibility to lowering surface tension σ and could vary with Γ, depending on the bulk surfactant concentration C_0. While we are modelling superspreading that typically occurs at high surfactant concentrations above the critical micelle concentration (CMC), we actually will be dealing with a large change of Γ along the interface in the vicinity of the contact line. So β might also vary considerably. Nevertheless, we still choose a constant β to simplify our analysis based on the following rationales.

First of all, we notice that it is the interfacial concentration Γ that determines surface tension. So even at C_0 higher than the CMC, the surface tension changes are controlled by the interfacial concentration at around the CMC, Γ_{CMC}, which does not vary with C_0. Suppose that at a high C_0 abundant surfactant molecules are populated on the interface with the interfacial surfactant concentration Γ_0 (at an order of Γ_{CMC}) and the corresponding surface tension σ_0. If variations of Γ are not large, β can be approximated as a constant value $\beta_0 = -(\partial\sigma/\partial\Gamma)_0$ (which is generally small) corresponding to the above state. As will be shown in §§ 3 and 4, as long as the prescribed local surfactant leakage rate is low, Γ merely displays a little or moderate decrease from Γ_0 far away from the contact line. So in this outer region, because the dependence of σ on Γ is approximately linear, using $\beta \approx \beta_0$ in (2.2) can still faithfully describe the Marangoni stress behaviour in the region.

For the region near the contact line, however, because of the prescribed local surfactant leakage, there exists a small depletion region where Γ shows a very sharp decrease to the clean-interface state. In this depletion region, especially for the close proximity to the contact line, surfactant molecules are almost emptied out by the leak. So the interface thereof is little contaminated by surfactant having an averaged interfacial concentration Γ_1 much lower than $\Gamma_0 (\sim \Gamma_{CMC})$. Hence in this inner region, σ also varies linearly with Γ under a constant susceptibility $\beta_1 = -(\partial\sigma/\partial\Gamma)_1 \approx (\sigma_{clean} - \sigma_1)/\Gamma_1$ (where σ_{clean} is the clean-interface surface tension and σ_1 the surface tension corresponding to Γ_1). In other words, in both outer and inner regions, because surface tension changes are small, how σ varies with Γ in

https://doi.org/10.1017/jfm.2018.626 Published online by Cambridge University Press

each region can be approximately represented by a linear equation of state but with distinct values of β.

Despite the above, since the behaviour of σ actually deviates from two limiting surfactant states near which surface tension variations are small $-\Delta\sigma_0$ from the surfactant-crowded state and $\Delta\sigma_1$ from the clean-interface state, it might be conceivable that the characteristic surface tension changes $\Delta\sigma_0 = \beta_0\Gamma_0$ and $\Delta\sigma_1 = \beta_1\Gamma_1$ in these two regions are comparable in magnitude, i.e. $\beta_0\Gamma_0 \sim \beta_1\Gamma_1$ (so $\beta_1 \sim \beta_0\Gamma_0/\Gamma_1 \gg \beta_0$, which is typical for most surfactants). In this case, even using $\beta_0\Gamma_0$ in the outer region as a scale for the surface tension change in the inner region might not cause a qualitative change to the characteristics of the inner region. Hence, throughout this work, we take $\beta = \beta_0$ in (2.2) and use Γ_0 to be the characteristic interfacial concentration. In fact, as will become clear in our subsequent analysis, because it is the surface tension change near the contact line that matters and also because this change can be expressed in terms of the prescribed leakage flux, the resulting spreading speeds (3.17) and (4.14), which are our main results, will not explicitly depend on the actual value of β.

To fulfil the requirement of zero flow rate across the wedge, the pressure gradient has to satisfy

$$p_x = (3\eta/h^2)[\tau_s h/2\eta + U]. \tag{2.3}$$

The pressure here is supported by the Laplace pressure at the interface:

$$p = -\sigma h_{xx}. \tag{2.4}$$

Again, since the surfactant concentration here is located in the regime above CMC where superspreading occurs, σ does not vary significantly with Γ and hence can be roughly represented by σ_0. However, as will be seen in §§ 3 and 4, this approximation will break down in the close proximity of the contact line where surfactant molecules are almost emptied out by the prescribed local surfactant leakage. In this surfactant-devoid region, the clean-interface value σ_{clean} will be used in σ instead. As for the region sufficiently away from the contact line, the interface with $\sigma = \sigma_0$ remains virtually flat and hence $p \approx 0$. So even using $\sigma = \sigma_{clean}$ in (2.4) will not alter the characteristics for the region far away from the contact line. Also because (2.4) will be used to determine the actual dynamic contact angle due to the deformation of the almost clean part of the interface close to the contact line, we can approximate $\sigma \approx \sigma_{clean}$ in (2.4) for such an analysis, which will be implemented in §§ 3.3 and 4.2.

The remaining issue is to determine how Γ distributes along the interface. Because we look at the local surfactant transport in the vicinity of the contact line and also because it occurs at a much smaller length scale than the drop's, the associated time scale is typically much shorter than the drop spreading time scale. Hence, in the latter time scale, we can treat the surfactant transport at a quasi-steady state. This demands the net of the surface convection flux $u_s\Gamma$ to be equal to the diffusive flux J_D between the interface and the bulk phase:

$$[u_s\Gamma]_x = J_D, \tag{2.5}$$

where u_s is the velocity at the interface given by

$$u_s \equiv u(y = h) = \tau_s h/4\eta - U/2. \tag{2.6}$$

https://doi.org/10.1017/jfm.2018.626 Published online by Cambridge University Press

In (2.5), we assume that surface diffusion is negligible. As mentioned earlier in § 1, we model superspreading by prescribing a local surfactant leakage to set-up the required interfacial surfactant concentration gradient. So for soluble surfactant, J_D will be specified as a local diffusive flux across the wedge to model the transfer of surfactant from the interface toward the substrate (see § 4). As for insoluble surfactant, a constant surface flux J_s will be used to reflect the surfactant leaking effect through the contact line and the surfactant transport equation is then given by $u_s\Gamma = -J_s$, reduced from (2.5) with $J_D = 0$ (see § 3).

The main equations are (2.5) and (2.3). After substitution of (2.2), (2.4) and (2.6), we arrive at the following coupled set of equations for h and Γ:

$$[(\beta\Gamma_x h/\eta + 2U)\Gamma]_x = -4J_D, \tag{2.7}$$

$$\sigma h^2 h_{xxx} = (3/2)\beta\Gamma_x h - 3\eta U. \tag{2.8}$$

We non-dimensionalize the above equations with $z = x/L$, $H = h/\theta_0 L$, $G = \Gamma/\Gamma_0$, $j_D' = J_D L/u_M\Gamma_0$, $V = U/u_M$ and $\gamma = \theta_0^2(\sigma/\Delta\sigma_0)$. Here L is an appropriate length scale such that it is sufficiently long compared to the microscopic region (such as the precursor film) near the contact line, but only up to the extent that it can make connection to the macroscopic region (such as the drop) far away from the contact line. The value of $u_M = \theta_0\Delta\sigma_0/\eta$ is the characteristic Marangoni velocity scale due to surface tension variations in the scale of $\Delta\sigma_0 = \beta_0\Gamma_0$. As a result, equations (2.7) and (2.8) can be re-written in dimensionless form as

$$[(G_z H + 2V)G]_z = -4j_D', \tag{2.9}$$

$$\gamma H^2 H_{zzz} = (3/2)G_z H - 3V. \tag{2.10}$$

Below we will use the above equations to model superspreading for both insoluble and soluble surfactants.

3. Superspreading with insoluble surfactant

3.1. *Marangoni stress singularity due to weak surfactant leakage*

Because superspreading generally occurs at the early stage of spreading, if the amount of surfactant exchange with the bulk is small compared to the initial amount of the surfactant on the interface, the surfactant spreader might behave like an insoluble surfactant with $j_D' = 0$. Karapetsas *et al.* (2011) have shown in their simulations that superspreading can occur to insoluble surfactant through direct transfer of surfactant from the interface onto the substrate without having mass interchange with the bulk. Below we theoretically show that it is possible to realize superspreading with insoluble surfactant in principle. As will also be shown subsequently, although actual superspreaders are not insoluble, this part of the analysis is able to elicit key features of superspreading that will appear again in the more realistic situation using soluble surfactant in § 4.

At $j_D' = 0$, equation (2.9) leads to

$$[HG_z + 2V]G = 4j_s, \tag{3.1}$$

with boundary condition $G(z \to 1) = 1$. Here $j_s \equiv J_s/u_M\Gamma_0 = J_s\eta/\theta_0\Delta\sigma_0\Gamma_0 (>0)$ measures the strength of surfactant leakage relative to Marangoni convection. The actual strength of the leakage flux is represented by J_s, accounting for the surfactant

https://doi.org/10.1017/jfm.2018.626 Published online by Cambridge University Press

transfer from the interface to the substrate through the contact line. This flux must be balanced by the convective surface flux along the interface: $u_s\Gamma = -J_s$, the original dimensional form of (3.1) from an integration of (2.5) with $J_D = 0$. Assume that this surfactant leakage is small so that it can be sustained by a sufficiently high surfactant concentration away from the contact line. Then we can let $-J_s$ be a negative constant to represent a 'sink' constantly drawing interfacial surfactant molecules toward the contact line. As can also be clearly seen from (3.1), to establish $G_z > 0$ and hence the Marangoni stress $\Sigma \equiv -G_z < 0$ to aid in the contact line's advancement, it can only be achieved by a local surfactant leak with $j_s > 0$ (see also figure 1*a*).

However, the contact line's advection V term in (3.1) tends to sweep interfacial surfactant molecules toward the contact line. This leads to an accumulation of surfactant near the contact line and hence diminishes G_z established by the j_s term. So whether the resulting Marangoni stress can be established toward the contact line will be determined by the competition between these two terms. If the surfactant leakage is too slow ($j_s \ll V/2$), equation (3.1) reduces to $-G_z = 2V/H$, making $\Sigma > 0$ oppose the contact line motion. Obviously, it is impossible to have superspreading in this case.

A similar competition between surfactant depletion and contact line sweeping has been shown previously by Joanny (1989) and Karapetsas *et al.* (2011). In particular, Karapetsas *et al.* (2011) showed in their simulations that the drop spreading rate can be promoted at a sufficiently high *Pe* but not too high (see their figure 5), where *Pe* is the Péclet number measuring the strength of surface convection relative to surface diffusion in the interfacial surfactant transport. Requiring a large enough *Pe* to promote spreading by Marangoni stress is simply because a too small *Pe* will smooth out the surfactant concentration gradient by diffusion. On the other hand, if *Pe* gets too high, strong contact line sweeping will make surfactant accumulate at the contact line, which will slow down the spreading unless surfactant depletion is fast enough to reverse the trend.

In fact, to achieve superspreading, $j_s > V/2$ is necessary for preventing surfactant accumulation at the contact line. If the surfactant leakage is fast ($j_s \gg V/2$), equation (3.1) reduces to

$$HG_zG = 4j_s. \tag{3.2}$$

To determine G from (3.2), we use Voinov's approximation (Voniov 1976; Snoeijer 2006) by assuming the wedge shape H to be a slowly varying function with respect to the linear one:

$$H = z\Theta, \tag{3.3}$$

where $\Theta \equiv \theta/\theta_0$ measures the departure of the point slope $\theta = h/x$ from θ_0 and $|\Theta_z| \ll 1$. Because Θ varies slowly with z, G can be determined by a straightforward integration of (3.2):

$$G = [1 + (8j_s/\Theta) \times \ln(z)]^{1/2}. \tag{3.4}$$

This indicates that G increases with the distance z to the contact line until it reaches the far-field value at $z = 1$ (i.e. reaching the scale of the macroscopic length L where the interfacial surfactant concentration is nearly constant Γ_0). Since surfactant molecules are constantly leaking out through the contact line due to the leakage flux j_s, G has to decrease on approaching the contact line (i.e. decreasing z). It is clear that the larger j_s is, the stronger the leakage and hence the greater the reduction of G in the direction toward the contact line. As also indicated by (3.4), since G starts from a constant level away from the contact line, as its decline continues toward the

https://doi.org/10.1017/jfm.2018.626 Published online by Cambridge University Press

contact line, at some point G must eventually vanish. We call this point the complete depletion point at which $G(z^*) = 0$:

$$z^* = \exp(-\Theta^*/8j_s), \tag{3.5}$$

with $\Theta^* \equiv \Theta(z^*)$. Equation (3.5) indicates that $z^* \to 0$ as $j_s \to 0$, meaning that for a small value of j_s there must exist a small surfactant-free zone of size z^*.

Equation (3.4) yields the Marangoni stress as

$$\Sigma = -G_z = -(4j_s/\Theta) \times (1/z) \times [1 + (8j_s/\Theta) \times \ln(z)]^{-1/2}. \tag{3.6}$$

As a result, Σ will be acting toward the contact line and thereby promote the contact line advancement. Note that both (3.4) and (3.6) only hold up to the critical point z^* given by (3.5). Below this point, surfactant molecules are completely emptied out by the leak and hence the Marangoni stress vanishes. As also indicated by (3.5), the surfactant-free zone of size z^* will shrink very rapidly on lowering j_s. In other words, G with small j_s will exhibit a sharp decline near the contact line.

Now we inspect the behaviour of G and Σ given by (3.4)–(3.6). If the surfactant leakage in (3.1) is not too fast such that

$$2V \ll 4j_s \ll 1, \tag{3.7}$$

the surfactant-free zone will be small, i.e. $z^* \ll 1$. For z sufficiently far from z^*, the surfactant concentration varies slowly with z as $G \approx 1 + 4j_s \times \ln(z)$ (with $\Theta \approx 1$ in (3.4)), and hence the corresponding Marangoni stress behaves as $\Sigma \approx -4j_s \times 1/z$. However, for z close to z^*, $G \approx (1 - \ln(z)/\ln(z^*))^{1/2}$ (with $\Theta \approx \Theta^*$ in (3.4) together with (3.5)). This yields $\Sigma \approx (1/2\ln(z^*)) \times 1/z \times (1 - \ln(z)/\ln(z^*))^{-1/2}$, diverging much faster than the usual viscous stress singularity $1/z$ (Huh & Scriven 1971). As will be shown later, such Marangoni stress singularity will call for a new contact line structure that can account for the linear spreading law.

To confirm the features discussed above, we also solve (3.1) to determine the actual profiles of G and Σ. To better illuminate the singular nature for both G and Σ, we look at the outer region by taking $H = z$. This admits an analytical solution:

$$1 - G + (2j_s/V)\ln[(2j_s - V)/(2j_s - VG)] = 2V\ln(z). \tag{3.8}$$

Figure 2 plots both G and Σ profiles calculated from (3.8) at a fixed value of V with various values of j_s under the constraint (3.7). We also plot the asymptotic results (3.4) and (3.6) (with $\Theta = 1$), showing an excellent agreement with those given by (3.8). As shown in figure 2(*a*), for a given value of j_s, G declines as the distance z to the contact line decreases. Notice that G vanishes at some particular point, which exactly corresponds to the complete depletion point z^* – the lower j_s the smaller z^* in accordance with (3.5). On approaching z^*, such a decline in G gets sharper. For a very little surfactant leakage having $j_s = 0.01$ or lower, G shows merely a small decrease from the equilibrium value (i.e. $G = 1$) away from the contact line. But near the contact line, because the influence of the leak becomes perceivable, a small depletion region has to form in response to the leak, showing a very sharp decrease in G. Such a boundary-layer-like surfactant concentration profile also resembles the simulation result obtained by Karapetsas *et al.* (2011) for an insoluble surfactant (see their figure 3*a*). As for Σ, its magnitude is increased as z is decreased, and rises more sharply on approaching z^*, as displayed in figure 2(*b*). The value of Σ blows up as $z \to z^*$, signifying a Marangoni stress singularity. All these features confirm those given by (3.4)–(3.6).

https://doi.org/10.1017/jfm.2018.626 Published online by Cambridge University Press

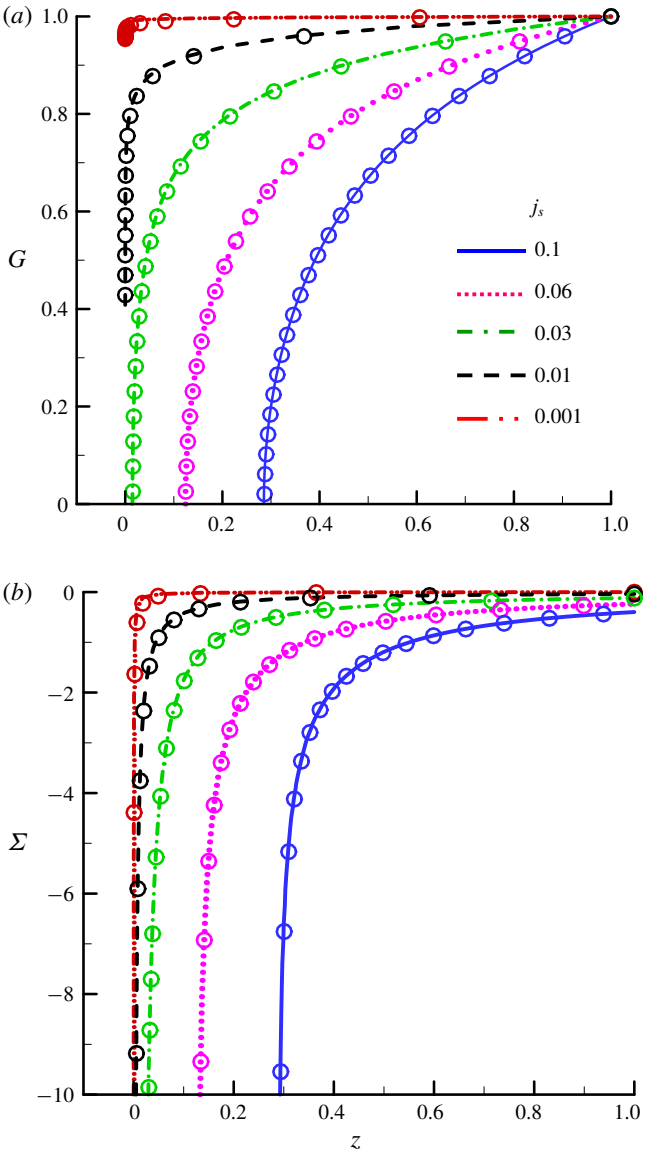


FIGURE 2. (Colour online) (*a*) Calculated surfactant distribution G for insoluble superspreader with various values of surfactant leakage flux j_s at $V = 0.001$. Lines: exact solution equation (3.8). Symbols: approximate solution equation (3.4). (*b*) Shows the corresponding Marangoni stress $\Sigma = -G_z$ whose exact and approximate values are evaluated using (3.1) and (3.6) respectively. All the results are calculated at $H = z$. G vanishes at the depletion point z^* near which rapid decline in G and divergence in Σ are evident.

3.2. *Emergence of a new contact line structure*

As indicated by (3.6), for small j_s, a Marangoni stress singularity can exist on approaching the contact line. Because it diverges at a much faster rate than the usual viscous stress singularity $1/z$, there is no way to dissipate it by the viscous force

https://doi.org/10.1017/jfm.2018.626 Published online by Cambridge University Press

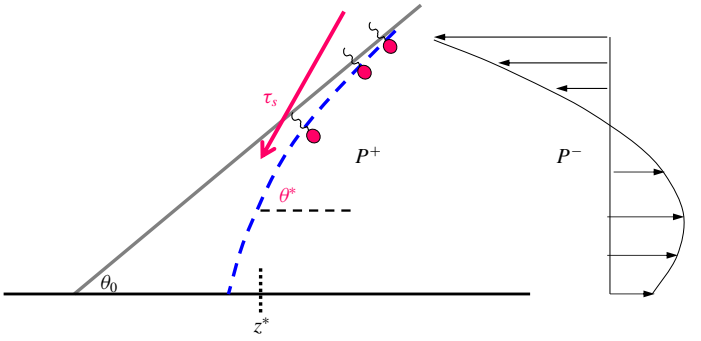


FIGURE 3. (Colour online) Schematic illustration of the interface profile and flow field near the contact line. Owing to surfactant leakage near the contact line, there exists a complete depletion point z^* below which there is no surfactant on the interface. The Marangoni shearing toward the contact line can lead to a pressure build-up, bending the interface into a microscopic capillary nose with dynamic contact angle θ^* greater than the apparent dynamic contact angle θ_0.

exerted by the substrate through the movement of the contact line (as it is derived under $j_s \gg V/2$ due to (3.7)). It thus follows that the dissipation of the Marangoni forcing has to be sought at the microscopic level at the scale comparable to or below z^*, implying that a new contact line structure must emerge, which is explained as follows.

According to (3.6), an intensified Marangoni stress $\Sigma = -G_z < 0$ is shearing the interface in the direction toward the contact line. From (2.10), this shearing will lead pressure $P = -\gamma H_{zz}$ to build up in the direction toward the contact line, i.e. $P_z > 0$. The mounting pressure near the contact line will in turn bend the air–liquid interface into a capillary nose (see figure 3), making the actual contact angle θ_{actual} greater than θ_0. Such bending of the interface with an increased dynamic contact angle is consistent with the small ridge at the moving front observed in the simulation study by Karapetsas *et al.* (2011) (see their figure 3*a*). Since it is the surfactant leakage responsible for $\Sigma < 0$ that bends the interface, θ_{actual} should mainly vary with j_s, regardless of the contact line speed U as long as (3.7) is satisfied. Apparently, the behaviour of θ_{actual} cannot be described by the classical clean-interface de Gennes–Cox–Voinov law that links the apparent dynamic contact angle to U (Voniov 1976; de Gennes 1985; Cox 1986*a*). Instead, a new wetting law must emerge to govern how θ_{actual} varies with j_s. Because of surfactant leakage and Marangoni stress, the physics involved in determining this new law will be very different from those in deriving the de Gennes–Cox–Voinov law. So we anticipate that the corresponding contact line structure will also be distinct from the latter's.

In fact, because the interface becomes clean below $x^*(= z^*L \ll L)$, the strong Marangoni shearing will transform into an enormous capillary pressure and this pressure will act as an additional wetting force to drive the contact line. The situation is quite distinct from the usual de Gennes–Tanner capillary wetting that occurs in a somewhat macroscopic sense over the outer length scale L (de Gennes 1985). In contrast, such capillary wetting takes place in a microscopic sense at the length scale x^*. More importantly, it is not purely driven by surface tension but by the Marangoni shearing set-up by the surfactant leakage near the contact line. It is this

https://doi.org/10.1017/jfm.2018.626 Published online by Cambridge University Press

local Marangoni-driven capillary wetting responsible for constant wetting speed and hence the linear spreading law seen in superspreading.

We should stress that the peculiar features mentioned above are the propositions that closely follow the two analytical results derived from our theory under the 'little but fast' leak condition (3.7): (i) the complete depletion point z^* given by (3.5), and (ii) the Marangoni stress singularity at z^* in (3.6). Although somewhat similar views can be drawn from the simulations by Karapetsas *et al.* (2011), here we will provide a rigorous proof for these propositions, which is given next.

3.3. *Marangoni-driven capillary wetting: a new dynamic contact angle relationship*

To determine the actual contact line speed caused by the Marangoni-driven capillary wetting described above, we need to establish the corresponding dynamic contact angle relationship. Hence we consider (2.10) by neglecting the V term under (3.7). Further combining (3.2), we arrive at

$$\gamma H^2 H_{zzz} = 6j_s/G. \tag{3.9}$$

Note here that the surface tension parameter $\gamma = \theta_0^2 \sigma_{clean}/\Delta\sigma_0$ is taken to correspond to the clean interface's tension σ_{clean}. This is because we want to determine the microscopic contact angle as z approaches the complete depletion point z^*, the pressure has to match that at z^*. Substituting (3.4) into (3.9) and writing H in terms of Θ using (3.3), (3.9) becomes

$$\Theta^2 \Theta_{zz} = 6\gamma^{-1} j_s \times z^{-2}[1 + (8j_s/\Theta) \times \ln(z)]^{-1/2}. \tag{3.10}$$

For the left-hand side of (3.10), we have used Voinov's approximation $H_{zzz} \approx \Theta_{zz}$ from $H_z = \Theta + z\Theta_z \approx \Theta$.

Equation (3.10) will be used to determine the actual contact angle θ_{actual}. Because z^* is small, θ_{actual} can be roughly represented by $\theta(z^*)$. Therefore, the purpose of solving (3.10) is to find $\Theta(z^*)$. Following the approach to solving the Bretherton equation for deriving the de Gennes–Cox–Voinov wetting law (see appendix A, § A.1), equation (3.10) can be solved approximately using Voinov's method (see appendix A, § A.2). Integrating both the left- and right-hand sides of (3.10) respectively and making use of the fact that $\int_1^z \Theta^2 \Theta_{zz}\,\mathrm{d}z \approx \Theta^2 \Theta_z$ (see (A 3) in appendix A), equation (3.10) becomes

$$\Theta^2 \Theta_z = 6\gamma^{-1} j_s \times \phi(z), \tag{3.11}$$

where $\phi(z)$ is the integral below (obtained by (A 11) in appendix A):

$$\phi(z) = \int_1^z z^{-2}[1 + (8j_s/\Theta) \times \ln(z)]^{-1/2}\,\mathrm{d}z \approx \ln(z). \tag{3.12}$$

Integrating (3.11) from $z = 1$ from $z = z^*$ and recognizing $\Theta(z = 1) = 1$ and $\int_1^{z^*} \ln(z)\,\mathrm{d}z \approx 1$ for small z^*, we obtain

$$\Theta^3(z^*) = 1 + 18\gamma^{-1} j_s. \tag{3.13}$$

With $\Theta(z^*) = \theta^*/\theta_0$, $\gamma = (\sigma_{clean}/\Delta\sigma_0)\theta_0^2$ and $j_s = J_s\eta/\Delta\sigma_0\theta_0\Gamma_0$, the slope θ^* at $z^*(\ll 1)$, which can represent the actual contact angle θ_{actual}, can be determined as

$$\theta^{*3} = \theta_0^3 + 18Ca_1. \tag{3.14}$$

https://doi.org/10.1017/jfm.2018.626 Published online by Cambridge University Press

Here, instead of the usual capillary number $Ca = \eta U/\sigma_{clean}$, equation (3.14) is characterized by the modified capillary number based on the speed of surfactant leakage J_s/Γ_0,

$$Ca_1 \equiv \theta_0^3 \gamma^{-1} j_s = (J_s/\Gamma_0)\eta/\sigma_{clean}. \tag{3.15}$$

Somewhat surprisingly, equation (3.14) looks quite similar to the well-known de Gennes–Cox–Voinov law (see (A 9) in appendix A). As θ^* in fact measures the slope of the 'capillary nose' which is surfactant free, it should match the clean-interface contact angle described by the de Gennes–Cox–Voinov law (see (A 9) in appendix A):

$$\theta_{clean}^3 \approx 9Ca \ln(z^*L/\ell). \tag{3.16}$$

Here the length scale ratio in the logarithmic term is taken as the length z^*L of the surfactant-free zone (with z^* given by (3.5)) to a microscopic cutoff length $\ell(\ll z^*L)$ or an inner length scale (due, for instance, to the precursor film ahead of the capillary nose or to wall slip). The associated microscopic contact angle $\theta(\ell)$ is assumed negligible here. Matching θ^* given by (3.14) to θ_{clean} given by (3.16), we can determine the contact line speed as

$$U = \frac{1}{9}\frac{\sigma_{clean}}{\eta}\theta_0^3(1 + 18\gamma^{-1}j_s)[\ln(z^*L/\ell)]^{-1}, \tag{3.17}$$

wherein $\ln(z^*) = -(1 + 18\gamma^{-1}j_s)^{1/3}/8j_s$ is a result of combining (3.5) and (3.13). For $18\gamma^{-1}j_s \sim O(1)$ or smaller (i.e. $18Ca_1 \sim O(\theta_0^3)$ or smaller), U scales as the capillary velocity $\theta_0^3\sigma_{clean}/\eta$, just like that of capillary wetting. Notice that during the spreading θ_0 is gradually decreasing whereas the surfactant leakage contribution $18Ca_1$ in (3.14) is kept constant. Because the ratio of the latter to θ_0^3 in (3.14) varies as θ_0^{-3}, the contribution from surfactant leakage $18Ca_1$ to θ^* would become increasingly important during the spreading. In other words, as long as $18\gamma^{-1}j_s$ is not too small compared to unity, θ^* might still be dominated by $18Ca_1$ from the surfactant leakage and hence might not change significantly during spreading. In fact, if $18\gamma^{-1}j_s$ is too small, the situation will reduce to the usual capillary wetting and there will be no superspreading at all, making (3.17) no longer applicable.

On the other hand, if surfactant leakage is sufficiently strong such that $18\gamma^{-1}j_s \gg 1$ (i.e. $18Ca_1 \gg \theta_0^3$), not only does the contact angle $\theta^* \approx (8Ca_1)^{1/3}$ become independent of θ_0 in (3.14), but also the contact line speed (3.17) reduces to

$$U = 2\left(\frac{J_s}{\Gamma_0}\right)[\ln(z^*L/\ell)]^{-1}. \tag{3.18}$$

It is essentially the speed of surfactant leakage J_s/Γ_0 which is constant and independent of θ_0. This speed comes from the surface flow set-up by the surfactant leakage near the contact line through $u_s\Gamma = -J_s$ which gives $u_s \sim -J_s/\Gamma_0$. This surface flow is sustained by the corresponding Marangoni shearing working with surface tension to push the contact line forward, making the contact line advance at a constant speed given by (3.18). Together with the fact that U with not too small $18\gamma^{-1}j_s$ also does not change significantly during spreading, U given by (3.17) can be deemed as a constant, thereby explaining the linear spreading law seen in superspreading.

https://doi.org/10.1017/jfm.2018.626 Published online by Cambridge University Press

4. Superspreading with soluble surfactant

4.1. *Surfactant leakage due to corner diffusion and corresponding Marangoni shearing*

Having analysed superspreading with an insoluble surfactant, we now move on to soluble surfactant which is more relevant to superspreading. A similar contact line structure can also form due to surfactant leakage around the contact line. But unlike direct surfactant transfer from the interface onto the substrate for insoluble surfactant, the surfactant transport (2.5) is driven by a bulk surfactant concentration gradient resulting from desorption of surfactant from the interface to the substrate (see figure 1*b*). This process establishes a corner diffusion flux $J_D = \mathcal{D}(C_1 - C_2)/h$ from the surfactant-rich interface at concentration C_1 toward the surfactant-poor substrate at concentration $C_2(<C_1)$, where $\mathcal{D}$ is the bulk diffusivity of surfactant. In the dimensionless form, this flux can be re-written as $j_D' = j_D/H$, where $j_D = (\mathcal{D}\Delta C/\theta_0\Gamma_0)/u_M = \eta\mathcal{D}(\Delta C/\Gamma_0)/\Delta\sigma_0\theta_0^2$ measures the strength of the corner diffusion flux relative to Marangoni convection and $\Delta C = C_1 – C_2$. Hence (2.9) becomes

$$[(G_z H + 2V)G]_z = -4j_D/H. \tag{4.1}$$

We again focus on the little but fast leak scenario:

$$2V \ll 4j_D \ll 1, \tag{4.2}$$

where Marangoni shearing toward the contact line can be established by a weak surfactant leakage without being mitigated by the contact line's sweeping. Under this condition, equation (4.1) reduces to

$$[G_z HG]_z = -4j_D/H. \tag{4.3}$$

Using Voinov's approximation (3.3): $H = z\Theta$ modulated by a slowly varying function $\Theta(z)$, G can be determined below by integrating (4.3) with $G(z \to 1) = 1$:

$$G = [1 - (4j_D/\Theta^2) \times (\ln(z))^2]^{1/2}, \tag{4.4}$$

with the corresponding compete depletion point

$$z^* = \exp(-\Theta^*/2j_D^{1/2}). \tag{4.5}$$

The Marangoni stress is then

$$\Sigma = -G_z = (4j_D/\Theta^2) \times (\ln(z)/z) \times [1 - (4j_D/\Theta^2) \times (\ln(z))^2]^{-1/2}. \tag{4.6}$$

For z close to z^*, since $\Theta \approx \Theta^*$, equation (4.4) behaves as $G \approx [1 - (\ln(z)/\ln(z^*))^2]^{1/2}$, exhibiting a very sharp decay near z^*. The corresponding Marangoni stress is $\Sigma \approx \ln(z^*) \times (\ln(z)/z) \times (1 - (\ln(z)/\ln(z^*))^2)^{-1/2}$, again diverging much faster than the viscous stress singularity $1/z$.

Figure 3 plots both G and Σ profiles by numerically solving (4.1) with $H = z$ under (4.2). Similar to figure 2 for insoluble surfactant, the larger j_D is the sharper the decrease for G and hence the greater build-up of Σ. The results also show an excellent agreement with the approximation solution (4.4) and (4.6) with $\Theta = 1$, confirming the sharp decline in G and the divergence in Σ near z^* due to weak surfactant transfer shown above. The boundary-layer-like profile for G also resembles the simulation result reported by Karapetsas *et al.* (2011) for soluble surfactant (see their figure 9*a*).

https://doi.org/10.1017/jfm.2018.626 Published online by Cambridge University Press

4.2. *New contact line structure and dynamic contact angle relationship*

To determine the dynamic contact angle relationship based on (4.6), we need (2.10) by neglecting the V term under (4.2):

$$\gamma H H_{zzz} = (3/2)G_z. \tag{4.7}$$

Substituting (4.6) into (4.7) and re-writing it in terms of Θ using $H = z\Theta$ and $H_{zzz} \approx \Theta_{zz}$, we arrive at

$$\Theta^3\Theta_{zz} = -(6\gamma^{-1}j_D) \times (\ln(z)/z^2) \times [1 - (4j_D/\Theta^2) \times (\ln(z))^2]^{-1/2}. \tag{4.8}$$

Following the procedures given by appendix A (see § A.3), to solve (4.8) we first integrate its left- and right-hand sides to yield

$$\Theta^3\Theta_z = -(6\gamma^{-1}j_D) \times \psi(z), \tag{4.9}$$

where $\psi(z)$ is the integral below (obtained by (A 13) in appendix A):

$$\psi(z) = \int_1^z (\ln(z)/z^2) \times [1 - (4j_D/\Theta^2) \times (\ln(z))^2]^{-1/2}\,\mathrm{d}z \approx (\ln(z))^2/2. \tag{4.10}$$

Integrating (4.9) from $z = 1$ to $z = z^*$ and knowing $\Theta(z = 1) = 1$ and $\int_1^{z^*} [\ln(z)]^2\,\mathrm{d}z \approx -2$ for small z^*, we arrive at

$$\Theta^4(z^*) = 1 + 24\gamma^{-1}j_D. \tag{4.11}$$

Compared to (3.13) for an insoluble superspreader, the last term due to surfactant leakage has the same dependence on surface tension and surfactant leakage flux. However, the power of Θ is different. The additional power comes from the corner diffusion term $-4j_D/H$ in (4.3). Re-writing (4.11) in terms of actual physical quantities, we obtain the following dynamic contact angle relationship for a soluble superspreader:

$$\theta^{*4} = \theta_0^4 + 24Ca_2, \tag{4.12}$$

characterized by the modified capillary number

$$Ca_2 \equiv \theta_0^4\gamma^{-1}j_D = (D\Delta C/\Gamma_0)\eta/\sigma_{clean}. \tag{4.13}$$

So the velocity here $D\Delta C/\Gamma_0$ can be interpreted as the velocity of the surface flow induced by the corner diffusion flux, as indicated by (4.3). Matching θ^* given by (4.12) to θ_{clean} with (3.16), the contact line speed is found to be

$$U = \frac{1}{9}\frac{\sigma_{clean}}{\eta}\theta_0^3(1 + 24\gamma^{-1}j_D)^{3/4}[\ln(z^*L/\ell)]^{-1}, \tag{4.14}$$

wherein $\ln(z^*) = -(1 + 24\gamma^{-1}\ j_D)^{1/4}/2j_D^{1/2}$ is a result of combining (4.5) and (4.11). Similar to (3.17) for an insoluble superspreader, U again scales as the capillary wetting velocity $\theta_0^3\sigma_{clean}/\eta$. Impacts of surfactant leakage are mainly reflected in $(1 + 24\gamma^{-1}j_D)^{3/4} = (1 + (D\Delta C/\Gamma_0)\eta/\sigma_{clean}\theta_0^4)^{3/4}$. So for $24\gamma^{-1}j_D \gg 1$, equation (4.14) is reduced to

$$U = \frac{1}{9}\frac{\sigma_{clean}}{\eta}\left(\frac{\eta D\Delta C/\Gamma_0}{\sigma_{clean}}\right)^{3/4}[\ln(z^*L/\ell)]^{\ -1}. \tag{4.15}$$

https://doi.org/10.1017/jfm.2018.626 Published online by Cambridge University Press

Again, U is independent of θ_0. But U will vary as the 3/4 power of the driving surface flow $D\Delta C/\Gamma_0$, in contrast to the insoluble surfactant result (3.18) in which U is linearly proportional to J_s/Γ_0. The reason for this difference is that the power of θ^* in (4.12) does not match that of θ_{clean} in (3.16) because of the additional corner diffusion term $-4j_D/H$ in (4.1).

A remark is worth making below concerning the spreading speed given by (4.14). Recall that the concentrated Marangoni stress near the contact line is a result of a tiny surfactant leakage imposed by our model to account for the effects of the surfactant transfer from the interface to the substrate. This feature also agrees with what Karapetsas *et al.* (2011) observed in their simulation study. And yet, because of the leak, the contact line is actually surfactant free. So this Marangoni stress does not drive the contact line directly. Instead, it transforms into an enormous Laplace pressure, which in turn drives the contact line in a clean-interface manner. It is this Marangoni-driven capillary wetting that drives superspreading, leading to a constant spreading speed given by (4.14) and why the resulting speed scales as the capillary velocity. It is also this reason why the spreading speed U does not directly depend on the Marangoni stress but on the leakage flux j_D.

4.3. *Criterion of superspreading*

Because only a certain class of surfactants can exhibit superspreading, this implies that, to be a superspreader, certain requirements have to be met. While the present analysis is made under the constraint (4.2), a superspreader must at least satisfy

$$2V < 4j_D < 1, \tag{4.16}$$

where $V = U/u_M$ and $j_D = (\mathcal{D}\Delta C/\theta_0\Gamma_0)/u_M$ with $u_M = \theta_0\Delta\sigma_0/\eta$. The criterion $4j_D < 1$ to ensure that surfactant leakage is weak so that the surfactant depletion zone can be confined in a small region near the contact line. On the other hand, the leak has to be sufficiently strong to establish the surfactant concentration gradient needed to push the contact line without being mitigated by the contact line's sweeping. This demands $2V < 4j_D$.

In addition to (4.16), we also need the following condition from (4.11) to ensure that the Marangoni flow is strong enough to bend the interface by making θ^* significantly deviated from θ_0 according to (4.12):

$$24\gamma^{-1}j_D > 1, \tag{4.17}$$

with $\gamma = \theta_0^2(\sigma_{clean}/\Delta\sigma_0)$. Hence, to satisfy both (4.16) and (4.17), j_D has to be within the following range under which superspreading might occur:

$$\gamma/24 < j_D < 1/4. \tag{4.18}$$

It is worth pointing out that to make (4.18) hold it is necessary to have $\gamma/24 > V/2$ so that $V/2 < j_D$ in (4.16) can be replaced by $\gamma/24 < j_D$. In fact, $\gamma/24 > V/2$ is equivalent to $V/\gamma = Ca_{clean}\theta_0^{-3} < 1/12$, meaning that surface tension force has to be sufficiently strong compared to the viscous force. We further notice that $j_D = (\mathcal{D}\eta\Delta C/\Gamma_0)/\theta_0^2\Delta\sigma_0$ is approximately proportional to the surfactant concentration C_0 because superspreading generally occurs in the high concentration regime above the CMC where the surface coverage Γ_0 is nearly constant. As will be illustrated later in § 5, the actual value of C_0 is close to the lower bound from $\gamma/24 < j_D$ in

https://doi.org/10.1017/jfm.2018.626 Published online by Cambridge University Press

(4.18). This underpins the need for a sufficiently strong surfactant leakage in driving the contact line with Marangoni shearing. Also because $j_D > \gamma/24 > V/2$ here, not only $j_D > V/2$ guarantees that the as-established surfactant concentration gradient is not diminished by the contact line's sweeping, but also $\gamma/24 > V/2$ ensures that the Marangoni shearing can turn into a capillary wetting force to drive the contact line.

On the other hand, if the surfactant leakage is too strong, Marangoni shearing would no longer be concentrated near the contact line to make the Marangoni–capillary mechanism work. In fact, in this case the entire interface would be short of surfactant, which reduces to the standard capillary wetting and hence does not lead to superspreading. This demands $1/4 > j_D$ to give the upper bound of C_0. All these requirements result in a range for C_0, restricting the surfactant concentration and properties for seeing superspreading.

To better see how the condition for seeing superspreading is determined by surfactant concentration, we re-write j_D in terms of the adsorption length $\lambda \equiv \Gamma_0/\Delta C$. This allows us to transform (4.18) to the following range for the dimensionless adsorption length $\Lambda \equiv \lambda\sigma_{clean}/\eta\mathcal{D}$:

$$\left(\frac{\sigma_{clean}}{\Delta\sigma_0}\right)\theta_0^{-1} < \frac{1}{4}\Lambda\theta_0 < 24\theta_0^{-4}. \tag{4.19}$$

In (4.19), the lower bound comes from $j_D < 1/4$ and the upper bound corresponds to $\gamma/24 < j_D$ in (4.18). In Λ, the diffusivity of surfactant molecule $\mathcal{D}$ can be evaluated using the Stokes–Einstein equation $\mathcal{D} = k_BT/6\pi\eta a$ with k_BT being the thermal energy and a the size of surfactant molecule. Hence Λ can be re-written as $\Lambda = 6\pi\lambda a\sigma_{clean}/k_BT$, measuring the amount of the work needed to spread a surfactant monolayer of thickness a over distance λ under the actions of surface tension σ_{clean}.

As indicated by (4.19), to be a superspreader, the adsorption length $\lambda \equiv \Gamma_0/\Delta C \sim \Gamma_0/C_0$, has to be within a certain range. Apparently, not every surfactant can meet this criterion. As λ essentially represents the adsorption isotherm of a surfactant, for a given surfactant and a given surface coverage Γ_0, equation (4.19) will fix the range of surfactant concentration C_0 in which superspreading will be observed. In addition, the range strongly depends on the apparent dynamic contact angle θ_0, suggesting that surfactant wettability and surface chemistry also have a part to play. As a potential candidate of superspreader has to fulfil all of the requirements listed above, this restrains the types of surfactants that become superspreaders.

Recall that (4.19) comes from the need for a local surfactant leakage under the flux constraint (4.18). It seems that an arbitrary surfactant can produce such a leakage effect, which actually is not true. The reason is that to meet (4.18), the surfactant might require a specific affinity and a special kinetic pathway to adsorb onto the substrate, so that the surfactant transfer from the interface to the substrate can occur at the desired level. And to acquire such affinity and sorption kinetics, it is also necessary for the surfactant to possess certain chemical properties or structure that favour such a very restrictive adsorption process. In other words, the special physical and chemical properties needed for being a superspreader are actually hidden in the local surfactant leakage flux imposed by the present hydrodynamic model. As superspreading can also be influenced by other factors such as dynamic surface tension (Rafai & Bonn 2005), evaporation (Semenov *et al.* 2013), wetting and surface chemistry (Ivanova, Zhantenova & Starov 2012), surfactant assembly (Stoebe *et al.* 1997; Kumar *et al.* 2003*a*), humidity (Ivanova *et al.* 2012), etc., the criterion (4.18) or (4.19) should be viewed as a part of the requirements for superspreading. Hence,

https://doi.org/10.1017/jfm.2018.626 Published online by Cambridge University Press

it is a sufficient condition for superspreading. That is, if this criterion is satisfied, superspreading might occur; but if superspreading occurs, then it must be fulfilled. Because we do not take into account all of these effects, to see superspreading, the range of surfactant concentration predicted by (4.19) would be wider than the actual concentration range occurring in experiments, which is indeed found in the case considered in the next section. Nevertheless, we at least verify that local surfactant leakage is one of the necessary elements for triggering superspreading.

5. Connections to experiments and simulations

Our analysis can capture a variety of results seen in experiments and simulations reported previously. Having established the criterion (4.19) for superspreading, we first estimate the range of surfactant concentration within which superspreading might occur experimentally. Assume $\Delta\sigma_0 \approx 2$ mN m^{-1} taken about 10 % of $\sigma_0 \approx 20$ mN m^{-1} (Rafai & Bonn 2005) (because near the contact line the interface is only a little contaminated by surfactant). With $\theta_0 \sim 10^{-1}$ and $\sigma_{clean} \approx 70$ mN m^{-1}, equation (4.19) yields $3.5 \times 10^3 < \Lambda/4 < 2.4 \times 10^6$. For $a \sim 1$ nm and $k_BT \approx 4 \times 10^{-21}$ J at 25 °C, the above range of Λ gives $\lambda = 45$ nm–30 μm. Since we stipulate that superspreading is driven by a local surfactant leakage through corner diffusion across the wedge (with soluble surfactant spreaders), to make this leaking process more effective, it might be more desirable to use high surfactant concentrations. In this case, the interface would likely be covered by densely packed surfactant molecules with the interfacial concentration Γ_0 as high as that at the CMC, Γ_{CMC} (which is nearly the maximum surface coverage that does not change beyond CMC). Hence, $\lambda \equiv \Gamma_0/\Delta C$ can be approximated as Γ_{CMC}/C_0 with C_0 being the surfactant concentration. With $\Gamma_{CMC} \sim 10^{-10}$ mol cm^{-2} and $C_{CMC} \sim 10^{-7}$ mol cm^{-3} for typical trisiloxane superspreaders (Kumar *et al.* 2003*b*), $\lambda = 45$ nm–30 μm yields C_0 that falls in the range of 10^{-8}–10^{-5} mol cm^{-3}. It is approximately 1/10–100 times C_{CMC}. In the experimental study by Rafai *et al.* (2002), superspreading was observed at $C_0 = 10$–$50C_{CMC}$, which falls into the range estimated above.

As for the spreading speed U, because superspreader surfactants are typically soluble, U can be roughly estimated as the capillary wetting velocity $\theta_0^3\sigma_{clean}/9\eta$ according to (4.14). With $\sigma_{clean} \approx 70$ mN m^{-1}, $\eta \approx 1$ m Pa s and $\theta_0 \sim O(10^{-1})$, we find $U \sim 1$ mm s^{-1} in agreement with experimental observations (Nikolov *et al.* 2002; Rafai *et al.* 2002; Wang *et al.* 2013; Nikolov & Wasan 2015). Using (4.14), we can see how U (in mm s^{-1}) varies with j_D, as displayed in figure 5. With $\sigma_{clean} \approx 70$ mN m^{-1}, $\Delta\sigma_0 \approx 2$ mN m^{-1}, $\theta_0 \sim 10^{-1}$ and $z^*L/\ell \sim 10^2$ (by taking 1 % of the typical value $L/\ell \sim 10^4$), to have U be of the order of mm/s observed in experiments, figure 5 reveals that the strength of the surfactant leakage is $0.02 < j_D < 0.2$, which also falls within $\gamma/24 < j_D < 1/4$ given by (4.18). This also confirms that a fraction of surfactant leakage will suffice to sustain the Marangoni-driven capillary wetting mechanism needed for superspreading.

The need for surfactant transfer from the interface to the substrate or local surfactant leakage to trigger superspreading implies that a special sorption kinetics is necessary to be a superspreader. Why such a characteristic is essential to a superspreader seems to have been partially supported by the experimental study of Rafai & Bonn (2005). These authors measured the dynamic surface tension for a trisiloxane superspreader and compared with that of a normal surfactant (dioctyl sulfosuccinate sodium salt, AOT) whose spreading does not deviate much from Tanner's law. Both measurements were conducted near the CMC using pendant drop and maximum bubble pressure

https://doi.org/10.1017/jfm.2018.626 Published online by Cambridge University Press

methods. Their results reveal that the differences between these two surfactants are rather striking (see their figure 4). In the normal surfactant case, the surface tension merely exhibits a slight decrease around 30 mN m^{-1} and quickly reaches an equilibrium (within 1 s). In contrast, the trisiloxane's surface tension shows a large change from the nearly clean-interface value 70 mN m^{-1} to the CMC value 22 mN m^{-1} but is slowly decreasing with time (in a period of 100 s). The much larger and slower change in the dynamic surface tension for the trisiloxane case indicates that trisiloxane surfactants would take a longer time to absorb onto the bubble/drop surface than normal surfactants. This implies that trisiloxane surfactants have less inclination to land onto an air–liquid interface compared to normal surfactants. If spreading a trisiloxane surfactant to a substrate that has some degree of affinity to the surfactant, the surfactant would be more inclined to absorb onto the substrate and hence even discourage the surfactant from adsorption onto the interface. Because the closer to the contact line the stronger the surfactant adsorption toward the substrate, the more severe surfactant deficiency would occur at the interface near the contact line, acting as if there were an additional sink to remove the surfactant. This in turn would establish a local Marangoni shearing toward the contact line to aid in its motion. But for normal surfactants, since they can be quickly absorbed onto an air–liquid interface and lack an adsorption bias to a solid substrate, they are not able to generate a local surfactant leakage to establish the Marangoni stress needed for speeding up the contact line advancement. In short, the peculiar dynamic surface tension behaviour of trisiloxane surfactant seen in the experiment by Rafai & Bonn (2005) can be linked to the notion of local surfactant leakage in our model for superspreading. Hence, the distinctions between superspreaders and normal surfactants are actually implied in the presupposition of local surfactant leakage used in our model.

Rafai *et al.* (2002) conducted their experiment for $C_0 = 0.8$–$50C_{CMC}$ and found that the spreading exponent can vary between 0.16 and 1, depending on C_0. At $C_0 = 10$–$50C_{CMC}$ the linear spreading law can be observed (see figure 6*a*). This concentration range corresponds to $\lambda = 200$ nm–1 μm, falling within $\lambda =$ 45 nm–30 μm estimated from (4.19). For C_0 below $10C_{CMC}$, however, the spreading is slowed down and the spreading exponent decreases on lowering C_0. At $C_0 = 0.8C_{CMC}$, which is the lowest surfactant concentration in their experiment, in particular, the spreading is the slowest, showing that the spreading radius R is growing as a 1/6 power of time (see figure 6*b*).

Various spreading power laws can be explained by the fact that surface tension gradients no longer occur locally near the contact line but are established over the drop radius R. In other words, the spreading is driven by a global Marangoni force. Balancing this force to the viscous force from (1.1), we get $U \sim \beta h \Delta\Gamma/\eta R \propto \Delta\Gamma/R^3$ (because $h \propto R^{-2}$ for fulfilling the constant drop volume constraint). Here $\Delta\Gamma$ is controlled by the amount of the surfactant over the drop surface, $\Gamma R^2 \sim M_i - qt$ with M_i being the initial amount of the interfacial surfactant and q the surfactant leakage rate due to the surfactant transfer/leak to the bulk/substrate.

At low C_0, q is small. So the surfactant might behave like an insoluble surfactant with $\Delta\Gamma \propto R^{-2}$, giving $U \propto R^{-5}$ and hence $R \propto t^{1/6}$. This explains the smallest spreading power 1/6 observed by Rafai *et al.* (2002).

At C_0 higher than the CMC, we have to consider impacts of $q \sim (J_b R^2 + J_s R)$ that comprise the surfactant flux to the bulk J_b and the leakage flux J_s at the contact line. In this case, the surface concentration varies as $\Delta\Gamma \sim qt/R^2$, giving $U \propto qt/R^5$. The spreading dynamics for this case is determined by how q varies with R, depending on whether J_b is diffusion controlled or kinetics controlled.

https://doi.org/10.1017/jfm.2018.626 Published online by Cambridge University Press

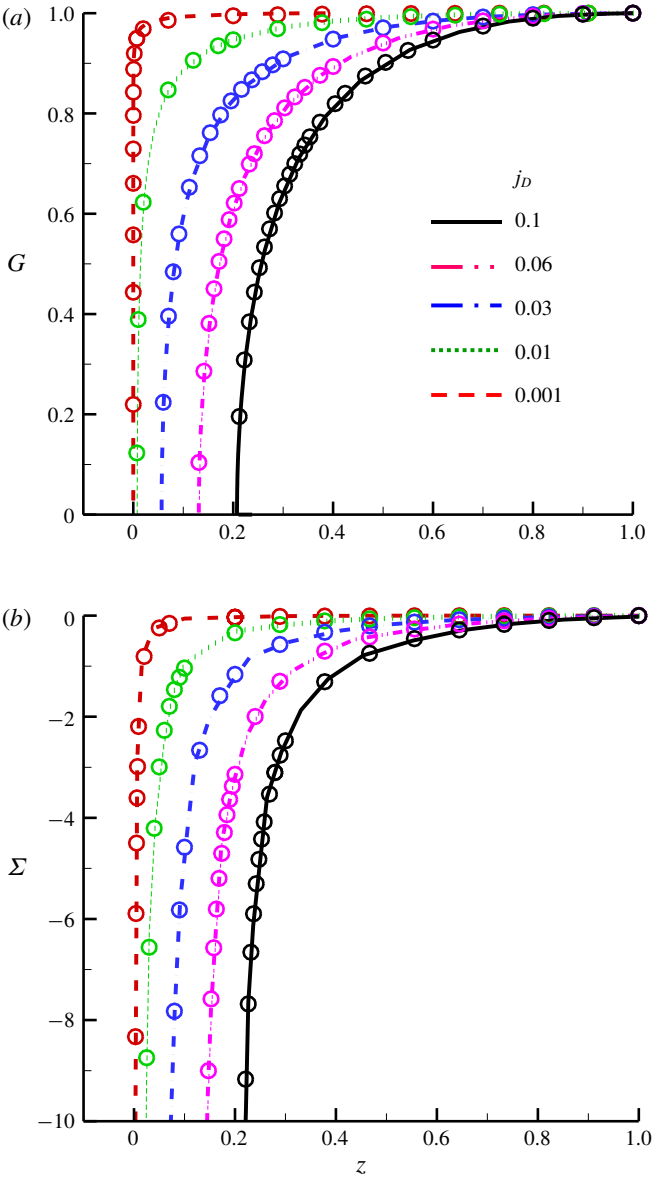


FIGURE 4. (Colour online) (*a*) Calculated surfactant distribution G for soluble superspreader with various values of corner diffusion flux j_D at $V = 0.001$. Lines: numerical solution to (4.1). Symbols: approximate solution (4.3). (*b*) Shows the corresponding Marangoni stress $\Sigma = -G_z$ whose exact and approximate values are evaluated using (4.1) and (4.6) respectively. All of the results are calculated at $H = z$. G vanishes at the depletion point z^*. Similar to figure 2 for an insoluble superspreader, rapid decline in G and divergence in Σ can also occur near z^*.

When C_0 is slightly higher than the CMC, q could be dominated by J_sR or controlled by lateral diffusion with $J_b \propto R^{-1}$. This leads to $q \propto R$ and hence $U \propto t/R^4$, giving $R \propto t^{2/5}$.

https://doi.org/10.1017/jfm.2018.626 Published online by Cambridge University Press

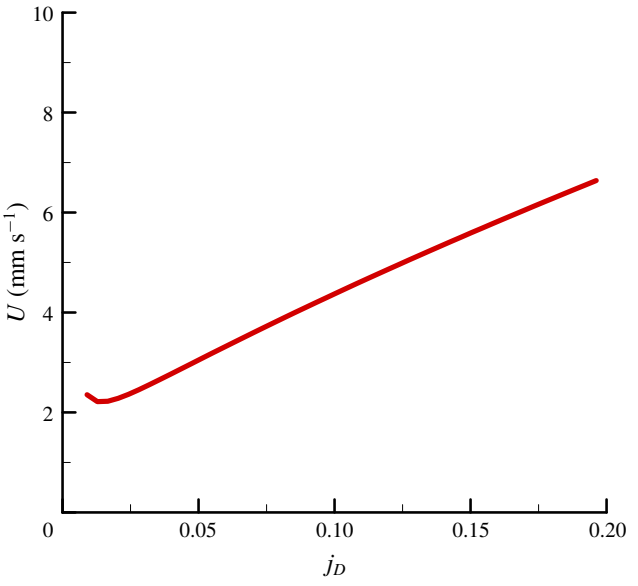


FIGURE 5. (Colour online) Dependence of actual wetting speed U on the surfactant transfer rate j_D for soluble superspreader. The result is obtained from (4.14) with $\sigma_{clean} \approx 70$ mN m^{-1}, $\Delta\sigma_0 \approx 2$ mN m^{-1} (approximately 10 % of $\sigma_0 \approx 20$ mN m^{-1}), $\theta_0 \approx 10^{-1}$ and $L/\ell \approx 10^4$.

At C_0 much higher than the CMC, q might be dominated by $J_b R^2$. Because J_b is likely kinetics controlled, it is roughly constant, especially at the late stage of spreading where plenty of surfactant molecules are absorbed onto the substrate or the interface. This leads to $q \propto R^2$ and hence $\Delta\Gamma \propto t$ as assumed by Nikolov & Wasan (2015). As a result, $U \propto \Delta\Gamma/R^3 \propto t/R^3$, giving $R \propto t^{1/2}$. This 1/2 power law has been observed during the late-time spreading in the experiment by Nikolov & Wasan (2015) (see figure 7).

It is possible that J_b is dominated by vertical diffusion with $J_b \propto h^{-1}$. This can happen when the transport is driven by the surfactant transfer from the interface to the substrate. Because this flux is most amplified near the contact line, this is essentially equivalent to the corner diffusion analysed in § 4. So $J_b \propto h^{-1} \propto R^2$ yields $q \sim J_b R^2 \propto R^4$. Together with $\Delta\Gamma \sim qt/R^2$, we arrive at $U \propto \Delta\Gamma/R^3 \propto t/R$, recovering the linear spreading law $R \propto t$. Together with the fact that the initial spreading in this case is also superspreading at constant U, this explains why the linear spreading law somewhat persists as it emerges, as Rafai *et al.* (2002) observed. The linear spreading law followed by the 1/2 power law observed by Nikolov & Wasan (2015) (see figure 7) suggests that the surfactant transport might undergo a transition from corner diffusion to kinetics controlled.

Likewise, for two-dimensional spreading with surfactant, we can also find the corresponding spreading laws in accordance with those reported previously. In this case, the drop width W expands under constraints $h \propto W^{-1}$ and $\Gamma \sim (M_i - qt)/W$ with $q \sim (J_b W + J_s)$. Also because the spreading speed now varies like $U \sim \beta h \Delta\Gamma/\eta W \propto \Delta\Gamma/W^2$, the resulting spreading dynamics will be different from three-dimensional cases.

When q is small at low C_0, because $\Delta\Gamma \propto W^{-1}$, we get $U \propto W^{-3}$ and hence $W \propto t^{1/4}$. This can occur after the linear superspreading law $W \propto t$, as seen in

https://doi.org/10.1017/jfm.2018.626 Published online by Cambridge University Press

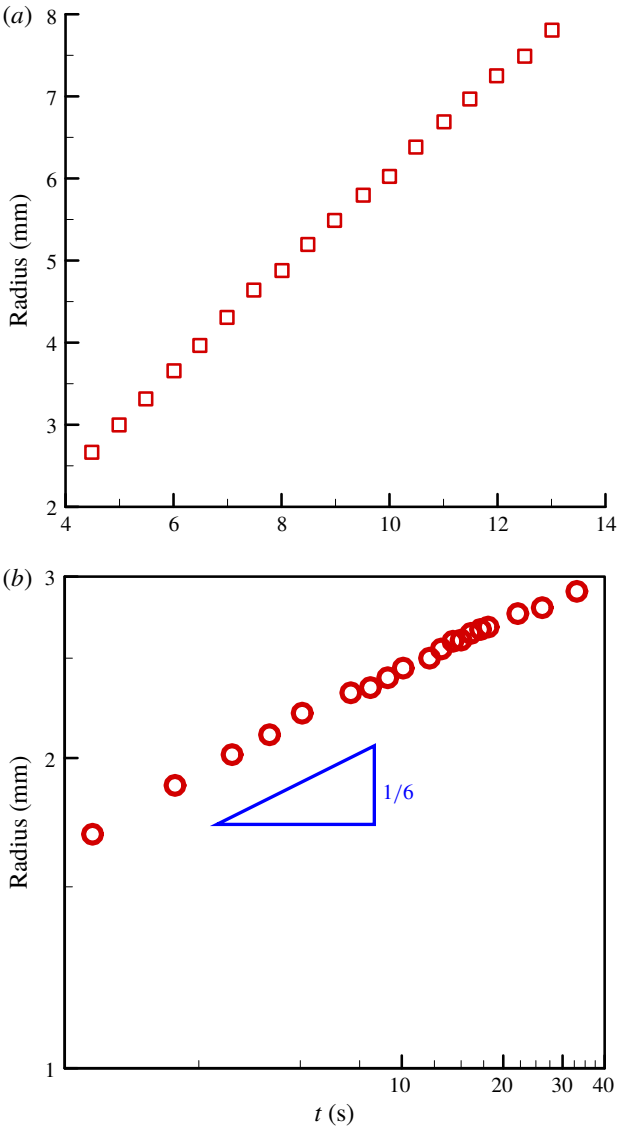


FIGURE 6. (Colour online) Experimental data by Rafai *et al.* (2002). (*a*) At surfactant concentration $C_0 = 10$–50 CMC, linear spreading law can be observed. (*b*) At $C_0 = 0.8$ CMC however, which is the lowest surfactant concentration in the experiment, the spreading radius grows as the $1/6$ power of time. The $1/6$ spreading exponent is the smallest in their experiment.

simulations for insoluble surfactant (Karapetsas *et al.* 2011). In the high C_0 regime, effects of q have to come into play. Because $\Delta\Gamma \propto qt/W$, we have $U \propto qt/W^3$, giving $W \propto (qt^2)^{1/4}$. If q is dominated by J_s or controlled by lateral diffusion with $J_b \propto W^{-1}$, q is roughly constant and we arrive at $W \propto t^{1/2}$. If q is dominated by corner diffusion with $J_b \propto h^{-1}$, the linear superspreading law $W \propto t$ is recovered. At late times the surfactant transport could be controlled by lateral diffusion again, making the spreading slow down to $W \propto t^{1/2}$. Such a transition from the linear law to

https://doi.org/10.1017/jfm.2018.626 Published online by Cambridge University Press

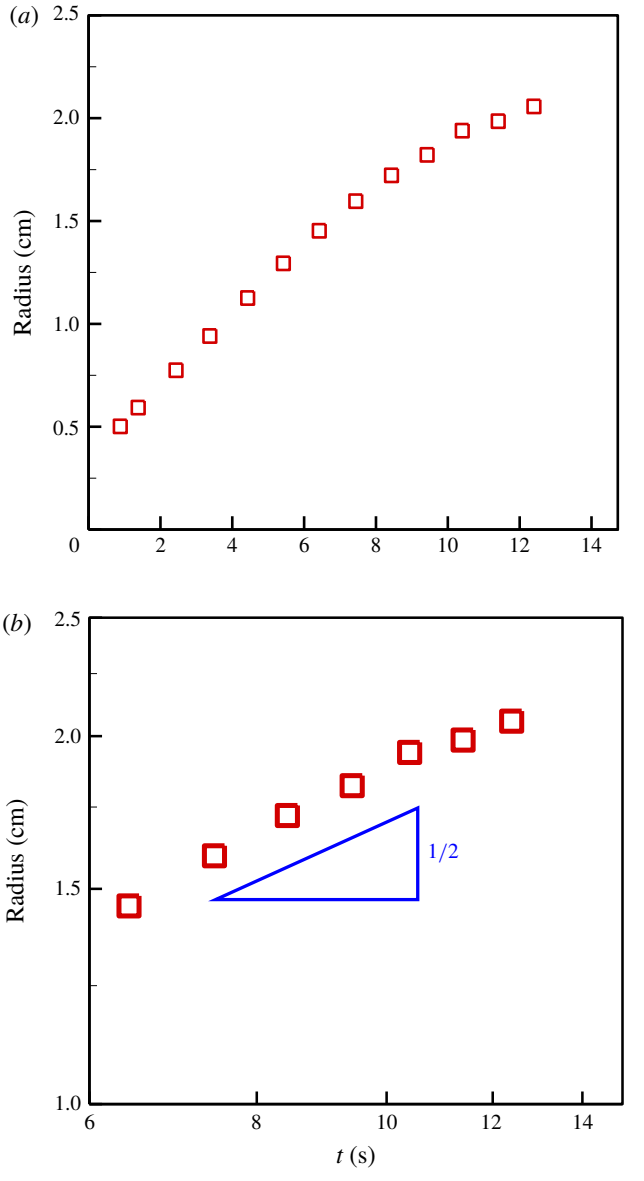


FIGURE 7. (Colour online) Experimental data by Nikolov & Wasan (2015). The spreading first follows the linear law as shown in (*a*). At late times it then slows down to the 1/2 law, as displayed in (*b*).

the 1/2 law has been observed by Karapetsas *et al.* (2011). On the other hand, if q is kinetics controlled and dominated by J_bW (with constant J_b), then $W \propto t^{2/3}$, which explains the main finding reported by Beacham *et al.* (2009).

In short, for three-dimensional (3-D) axisymmetric drop spreading with surfactant, its spreading dynamics follows $R \propto t^{\alpha}$ with $\alpha = 1/6 - 1$. Similarly, for two-dimensional (2-D) spreading we find $W \propto t^{\alpha}$ with $\alpha = 1/4 - 1$. Table 1 summarizes the various spreading laws shown above.

https://doi.org/10.1017/jfm.2018.626 Published online by Cambridge University Press

	Three-dimensional: $R \propto t^{\alpha}$	Two-dimensional: $W \propto t^{\alpha}$
Small q	1/6	1/4
$q \sim J_s R$	2/5	—
$q \sim J_s$	—	1/2
$q \sim J_b R^2$	1/2	—
$q \sim J_b W$	—	2/3
$J_b \propto h^{-1}$	1	1

TABLE 1. Various values of spreading exponent α for 3-D spreading and 2-D spreading with surfactant.

6. Analogous thermocapillary spreading

The present superspreading with surfactant can be analogous to thermocapillary spreading because both are driven by surface tension gradients. A similar Marangoni enhancement can also occur to thermocapillary spreading on a cooled plate (Ehrhard & Davis 1991; Ehrhard 1993; Smith 1995; Sui & Splet 2015). Such thermally driven spreading can also display a linear spreading law but it is achieved by nonlinear surface tension variations arising from a temperature minimum inside the droplet (Karapetsas *et al.* 2014; Chaudhury & Chakraborty 2015). If surface tension still varies linearly with temperature as commonly assumed, the situation would be quite similar to the present surfactant-driven spreading using a linear equation of state. In this case, we find that the same 1/6 and 1/2 spreading laws can emerge, depending on the cooling rate.

Similar to surfactant-driven spreading, a drop in this case will spread at speed $U_T \sim h\beta_T K_T/\eta$ driven by the gradient $K_T \equiv \partial_x T_s$ of the interfacial temperature $T_s = T_\infty - (T_\infty - T_w)/(1 + Bh/d)$ (Ehrhard & Davis 1991). Here $B = h_{air} d/k_{drop}$ is the Biot number measuring the heat flux on the air side (having heat transfer coefficient h_{air}) relative to that on the fluid side (having thermal conductivity k_{drop}), d is the scale of the drop height, T_w the plate temperature and T_∞ the ambient air temperature, and $\beta_T = -(\partial\sigma/\partial T)$.

When B is small, this describes the insulated limit, resembling spreading with insoluble surfactant. In this case, because $\Delta T_s \equiv T_s - T_\infty \propto h$, we get $U_T \propto hK_T \propto h\partial_x h \propto h^2/R \propto R^{-5}$ and hence arrive at $R \propto t^{1/6}$, similar to the late-time spreading of the insoluble superspreader shown in figure 6(*b*). This 1/6 spreading law is also supported by the experimental data measured by Ehrhard (1993), as shown in figure 8.

On the contrary, large B corresponds to the perfectly conducting limit, analogous to the spreading with soluble surfactant. Because this case has $\Delta T_s \propto h^{-1}$ much greater than the small B case, the gradient $K_T \propto \partial_x h/h^2 \sim 1/(hR) \propto R$ increases with R instead of decreasing with R. The spreading speed thus behaves as $U_T \propto hK_T \propto R^{-1}$. This results in $R \propto t^{1/2}$, similar to the late-time spreading of soluble superspreader shown in figure 7.

7. Concluding remarks

In conclusion, we have demonstrated that the curious linear superspreading law observed in experiments (Rafai *et al.* 2002; Nikolov & Wasan 2015) can be explained by the new contact structure resulting from a local surfactant leakage to the substrate near the contact line. As some affinity to the substrate is necessary for a surfactant superspreader, the rate of surfactant leakage represents the ability to

https://doi.org/10.1017/jfm.2018.626 Published online by Cambridge University Press

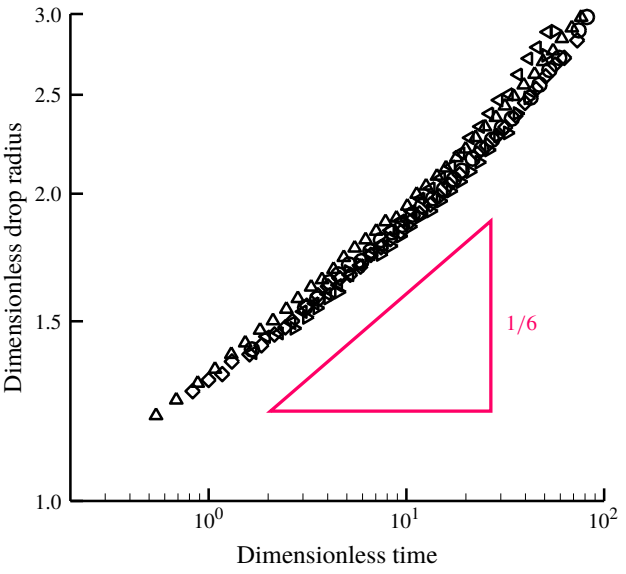


FIGURE 8. (Colour online) Experimental data by Ehrhard (1993). The same 1/6 law seen in figure 6(*b*) can also occur to the analogous thermocapillary on a cooled plate.

transfer surfactant to the substrate. We identify that a tiny rate of surfactant leakage will suffice to trigger superspreading. Specifically, a small surfactant depletion zone can form to almost remove interfacial surfactant molecules near the contact line. As a result, a concentrated Marangoni shearing can be established toward the contact line, exhibiting a Marangoni stress singularity diverging at a rate much faster than the usual viscous stress singularity (Huh & Scriven 1971). And more importantly, being devoid of surfactant near the contact line, this strong Marangoni shearing can turn into a local capillary force to drive the contact line in a surfactant-free manner. The actual dynamic contact angle depends only on the properties (i.e. affinity and concentration) of a surfactant spreader, giving a constant spreading speed according to the de Gennes–Cox–Voinov law and hence the linear spreading law independent of the extent of spreading. As such, we demonstrate that a rational account for superspreading can be made in a purely hydrodynamic manner without appealing to a specific surfactant structure or sorption kinetics. Our results also capture many features seen in the simulation study by Karapetsas *et al.* (2011).

It actually turns out that the condition for the occurrence of superspreading is quite stringent. On the one hand, the contact line movement can advect surfactant molecules toward the contact line to diminish the surface tension gradient established by the surfactant leakage. So if the rate of surfactant leakage is too low compared to the speed of the moving contact line, the spreading will be opposed by Marangoni retardation. On the other hand, the rate of surfactant leakage cannot be too high either; otherwise the drop would become virtually clean and its spreading would be governed by Tanner's 1/10 law. Even if there is a surfactant concentration gradient, it would no longer be confined near the contact line but extend over the drop, making Marangoni shearing less stronger than that in the tiny surfactant leakage case. Therefore, there must exist a range of the surfactant leakage rate within which superspreading can occur. We also convert this rate range in terms of surfactant concentration (see (4.19)).

https://doi.org/10.1017/jfm.2018.626 Published online by Cambridge University Press

This might explain the existence of a maximum spreading rate in a range of surfactant concentration (Hill 1988; Stoebe *et al.* 1996, 1997; Wang *et al.* 2013). The estimated surfactant concentration range is found to cover concentrations much higher than the CMC, just like the condition for seeing superspreading experimentally observed by Rafai *et al.* (2002). This explains why only a certain class of surfactants such as trisiloxane can serve as superspreaders.

Experiments show that the spreading of surfactant spreaders can be slowed down to a variety of powers of time (Rafai *et al.* 2002; Nikolov & Wasan 2015). We show that a variety of power laws can be attributed to distinct surfactant transport mechanisms governing at different surfactant concentration levels. In particular, the $1/6$ and the $1/2$ power laws found respectively by Rafai *et al.* (2002) and Nikolov & Wasan (2015) can occur to the analogous thermocapillary spreading processes. The same $1/6$ power law seen in the surfactant spreading experiment by Rafai *et al.* (2002) can appear in the thermocapillary spreading experiment by Ehrhard (1993). These resemblances between surfactant-driven spreading and thermocapillary spreading reverberate the ubiquitous role of the Marangoni effect in these dynamic wetting phenomena driven by non-uniform surface tension.

Acknowledgements

This work is supported by the Ministry of Science and Technology of Taiwan. The author would like to thank T.-I. Lin and Y.-S. Liu for preparing figures.

Appendix A. Voinov's method for solving Bretherton-like equations

The equations we are tackling can be generalized as of Bretherton type:

$$H^n H_{zzz} = f_1(z), \tag{A 1}$$

where f_1 is a given function and the power $n > 0$. The solution to (A 1) can be approximately determined using the approach below due to Voniov (1976) and Snoeijer (2006).

The essence of this method is that H is assumed to vary slowly with respect to z: $H = z\Theta$ with $|\Theta_z| \ll 1$. Because $H_z = \Theta + z\Theta_z \approx \Theta$, $H_{zzz} \approx \Theta_{zz}$. Hence (A 1) becomes

$$\Theta^n \Theta_{zz} = f(z), \tag{A 2}$$

with $f(z) = f_1(z)/z^n$.

The solution to (A 2) can be obtained by integrating (A 2) twice with the slow variation approximation for Θ. The first step is to take respective integration for the left- and right-hand sides of (A 2). Integrating the left hand side gives

$$\int_1^z \Theta^n \Theta_{zz}\,\mathrm{d}z = \Theta^n \Theta_z - \frac{1}{n+1}\int_1^z \Theta^{n-1}\Theta_z^2\,\mathrm{d}z \approx \Theta^n \Theta_z, \tag{A 3}$$

where we have used $\Theta_z(z \to 1) \to 0$ (*viz.*, $H_{zz}(z \to 1) \to 0$) and neglected the second term containing Θ_z which is assumed small here. Let the result of integrating the right-hand side of (A 2) be $\int_1^z f dz \equiv F(z)$. Then (A 2) reduces to

$$(\Theta^{n+1})_z = (n+1)F(z). \tag{A 4}$$

So the solution can be readily found by integrating both the left- and right-hand sides of (A 4).

https://doi.org/10.1017/jfm.2018.626 Published online by Cambridge University Press

A.1. *Derivation of the de Gennes–Cox–Voinov law for capillary wetting*

The approach described above can be used to solve (3.9) and (4.7) in the presence of surfactant. Prior to solving these equations, we validate this approach by first demonstrating its use for solving the Bretherton equation for complete capillary wetting: $h^2 h_{xxx} = -3Ca$ or

$$H^2 H_{zzz} = -3, \tag{A 5}$$

by letting $h = Ca^{1/3} LH(z)$ with $z = x/L$ (Bonn *et al.* 2009). Using $H = z\Theta$ with $|\Theta_z| \ll 1$ and $H_{zzz} \approx \Theta_{zz}$ (from $H_z = \Theta + z\Theta_z \approx \Theta$), equation (A 5) becomes

$$\Theta^2 \Theta_{zz} = -3/z^2. \tag{A 6}$$

Note that Θ in this case can be thought of as a rescaled slope in the sense that $h_x \approx Ca^{1/3}\Theta$. Following the derivation from (A 2) to (A 4), equation (A 6) can be reduced to

$$(\Theta^3)_z = 9/z, \tag{A 7}$$

which yields the solution

$$\Theta^3(z) = \Theta^3(z_1) + 9\ln(z/z_1). \tag{A 8}$$

Taking $z_1 = \ell/L$ associated with the inner length scale ℓ and replacing Θ by $\Theta \approx Ca^{-1/3} h_x$, equation (A 8) recovers the well-known de Gennes–Cox–Voinov law for the dynamic contact angle $\theta \approx h_x$ (Voniov 1976; de Gennes 1985; Cox 1986*a*):

$$\theta^3 = [\theta(\ell)]^3 + 9Ca\ln(x/\ell). \tag{A 9}$$

Having validated the use of Voinov's method in solving (A 6) for the standard capillary wetting problem, we next proceed to use it to solve the new equations (3.9) and (4.7) for modelling superspreading.

A.2. *Superspreading with insoluble surfactant*

For superspreading with insoluble surfactant, the equation is (A 2) by taking $n = 2$ and $f = Bz^{-2}[1 + A\ln(z)]^{-1/2}$ with $A = 8j_s/\Theta(\ll 1)$ and $B = 6\gamma^{-1} j_s$, as in (3.10). So an integration of f/B in (A 4) is $\phi(z)$ in (3.11):

$$\phi(z) = \int_1^z z^{-2}[1 + A\ln(z)]^{-1/2}\,\mathrm{d}z. \tag{A 10}$$

Let $\rho^2 = 1 + A\ln(z)$. Equation (A 10) changes to

$$\begin{aligned}\phi(z) &= (2/A)e^{1/A}\int_1^{\rho(z)} \exp(-\rho^2/A)\,\mathrm{d}\rho \\ &= (\pi/A)^{1/2} e^{1/A}(\mathrm{erf}(\rho(z)/\sqrt{A}) - \mathrm{erf}(1/\sqrt{A})) \approx \ln(z).\end{aligned} \tag{A 11}$$

The final result $\ln(z)$ comes from a Taylor expansion of the integral at $\rho = 1$. Integrating (3.11) from $z = 1$ to $z = z^*$ and recognizing that $\int_1^{z^*} \ln(z)\,\mathrm{d}z \approx 1$ for small z^*, the solution can be readily obtained, as given by (3.13).

https://doi.org/10.1017/jfm.2018.626 Published online by Cambridge University Press

A.3. *Superspreading with soluble surfactant*

For superspreading with soluble surfactant, we need to solve (4.7) or (A 2) with $n=3$ and $f=B(\ln(z)/z^2)\times[1-A(\ln(z))^2]^{-1/2}$ where $A=4j_D/\Theta^2(\ll 1)$ and $B=-6\gamma^{-1}j_D$. After integrating f in (A 4), we have to evaluate the following integral which is $\psi(z)$ in (4.9):

$$\psi(z)=\int_1^z(\ln(z)/z^2)\times[1-A(\ln(z))^2]^{-1/2}\,\mathrm{d}z. \tag{A 12}$$

Let $\rho^2=1-A(\ln(z))^2$. Equation (A 12) can be changed to the following integral which can be evaluated approximately by taking a Taylor expansion at $\rho=1$:

$$\begin{aligned}\psi(z) &= -A^{-1}\int_1^{(1-A(\ln(z))^2)^{1/2}}\exp(-A^{-1/2}(1-\rho^2)^{1/2})\,\mathrm{d}\rho\\ &\approx (-A^{-1})\times\exp(-A^{-1/2}(1-\rho^2)^{1/2})|_{\rho=1}\times(-A/2)\times(1-A(\ln(z))^2)^{-1/2}|_{z=1}\\ &\quad\times(\ln(z))^2\\ &\approx (\ln(z))^2/2.\end{aligned} \tag{A 13}$$

With (A 13), we can obtain the solution (4.11) by integrating (4.9) from $z=1$ to $z=z^*$ with $\int_1^{z^*}[\ln(z)]^2\,\mathrm{d}z\approx -2$ for small z^*.

REFERENCES

Beacham, D. R., Matar, O. K. & Craster, R. V. 2009 Wetting and surfactant-enhanced rapid spreading of drops on solid surfaces. *Langmuir* **25**, 14174–14181.

Bonn, D., Eggers, J., Indekeu, J., Meunier, J. & Rolly, E. 2009 Wetting and spreading. *Rev. Mod. Phys.* **81**, 739–803.

Chan, K. Y. & Borhan, A. 2006 Spontaneous spreading of surfactant-bearing drops in the sorption-controlled limit. *J. Colloid Interface Sci.* **302**, 374–377.

Chaudhury, K. & Chakraborty, S. 2015 Spreading of a droplet over a nonisothermal substrate: multiple scaling regines. *Langmuir* **31**, 4196–4175.

Chesters, A. K. & Elyousfi, A. B. 1998 The influence of surfactants on the hydrodynamics of surface wetting. I. Nondiffusing limit. *J. Colloid Interface Sci.* **207**, 20–29.

Clay, M. A. & Miksis, M. 2004 Effects of surfactant on droplet spreading. *Phys. Fluids* **16**, 3070.

Cox, R. G. 1986*a* The dynamics of spreading of liquids on a solid surface. Part 1. Viscous flow. *J. Fluid Mech.* **168**, 169–194.

Cox, R. G. 1986*b* The dynamics of spreading of liquids on a solid surface. Part 2. Surfactants. *J. Fluid Mech.* **168**, 195–220.

Ehrhard, P. 1993 Experiments on isothermal and non-isothermal spreading. *J. Fluid Mech.* **257**, 463–483.

Ehrhard, P. & Davis, S. H. 1991 Non-isothermal spreading of liquid drops on horizontal plates. *J. Fluid Mech.* **229**, 365–388.

de Gennes, P. G. 1985 Wetting: statics and dynamics. *Rev. Mod. Phys.* **57**, 827–863.

Hill, R. M. 1988 Superspreading. *Curr. Opin. Colloid Interface Sci.* **3**, 247–254.

Huh, C. & Scriven, L. E. 1971 Hydrodynamic model of steady movement of a solid/liquid/fluid contact line. *J. Colloid Interface Sci.* **35**, 85–101.

Ivanova, N. A., Zhantenova, Z. B. & Starov, V. M. 2012 Wetting dynamics of polyoxyethylene alkyl ethers and trisiloxanes in respect polyoxyethylene chains and properties of substrates. *Colloids Surfaces* A **413**, 307–313.

Jensen, O. E. & Grotberg, J. B. 1992 Insoluble surfactant spreading on a thin viscous film: shock evolution and film rupture. *J. Fluid Mech.* **240**, 259–288.

https://doi.org/10.1017/jfm.2018.626 Published online by Cambridge University Press

JENSEN, O. E. & NAIRE, S. 2006 The spreading and stability of a surfactant-laden drop on a prewetted substrate. *J. Fluid Mech.* **554**, 5–24.

JOANNY, J. F. 1989 Kinetics of spreading of a liquid supporting surfactant monolayer: repulsive solid surfaces. *J. Colloid Interface Sci.* **128**, 407–415.

KARAPETSAS, G., CRASTER, R. V. & MATAR, O. K. 2011 On surfactant-enhanced spreading and superspreading of liquid drops on solid surfaces. *J. Fluid Mech.* **670**, 5–37.

KARAPETSAS, G., SAHU, K. C., SEFIANE, K. & MATAR, O. K. 2014 Thermocapillary-driven motion of a sessile drop: effect of non-monotonic dependence of surface tension on temperature. *Langmuir* **30**, 4310–4321.

KIM, H.-Y., QIN, Y. & FICHTHORN, K. A. 2006 Molecular dynamics simulations of nanodroplet spreading enhanced by linear surfactants. *J. Chem. Phys.* **125**, 174708.

KUMAR, N., COUZIS, A. & MALDARELLI, C. 2003*b* Measurement of the kinetic rate constants for the adsorption of superspreading trisiloxanes to an air/aqueous interface and the relevance of these measurements to the mechanism of superspreading. *J. Colloid Interface Sci.* **267**, 272–285.

KUMAR, N., VARANASI, K., TILTON, R. D. & GAROFF, S. 2003*a* Surfactant self- assembly ahead of the contact line on a hydrophobic surface and its implications for wetting. *Langmuir* **19**, 5366–5373.

MALDARELLI, C. 2011 On the microhydrodynamics of superspreading. *J. Fluid Mech.* **670**, 1–4.

NIKOLOV, A. & WASAN, D. 2015 Current opinion in superspreading mechanisms. *Adv. Colloid Interface Sci.* **222**, 517–529.

NIKOLOV, A. D., WASAN, D. T., CHENGARA, A., KOCZO, K., POLICELLO, G. A. & KOLOSSVARY, I. 2002 Superspreading driven by Marangoni flow. *Adv. Colloid Interface Sci.* **96**, 325–338.

RAFAI, S. & BONN, D. 2005 Spreading of non-Newtonian fluids and surfactant solutions on solid surfaces. *Physica* A **358**, 58–67.

RAFAI, S., SARKER, D., BERGERON, V., MEUNIER, J. & BONN, D. 2002 Superspreading: aqueous surfactant drops spreading on hydrophobic surfaces. *Langmuir* **18**, 10486–10488.

RAME, E. 2001 The spreading of surfactant-laden liquids with surfactant transfer through the contact line. *J. Fluid Mech.* **440**, 205–234.

SEMENOV, S., TRYBALA, A., AGOGO, H., KOVALCHUK, N., ORTEGA, F., RUBIO, R. G., STAROV, V. M. & VELARDE, M. G. 2013 Evaporation of droplets of surfactant solutions. *Langmuir* **29**, 10028–10036.

SMITH, M. 1995 Thermocapillary migration of a two-dimensional liquid droplet on a solid surface. *J. Fluid Mech.* **294**, 209–230.

SNOEIJER, J. H. 2006 Free-surface flows with large slopes: beyond lubrication theory. *Phys. Fluids* **18**, 021701.

STAROV, V. M., DE RYCK, A. & VELARDE, M. G. 1997 On the Spreading of an insoluble surfactant over a thin viscous liquid layer. *J. Colloid Interface Sci.* **190**, 104–113.

STOEBE, T., LIN, Z., HILL, R. M., WARDS, M. D. & DAVIS, H. T. 1996 Surfactant-enhanced spreading. *Langmuir* **12**, 337–344.

STOEBE, T., LIN, Z., HILL, R. M., WARDS, M. D. & DAVIS, H. T. 1997 Enhanced spreading of aqueous films containing ethoxylated alcohol surfactants on solid substrates. *Langmuir* **13**, 7270–7275.

SUI, Y. & SPLET, P. D. M. 2015 Non-isothermal droplet spreading/dewetting and its reversal. *J. Fluid Mech.* **776**, 74–95.

TANNER, L. H. 1979 The spreading of silicone oil drops on horizontal surfaces. *J. Phys.* **12**, 1473.

THEODORAKIS, P. E., MÜLLER, E. A., CRASTER, R. V. & MATAR, O. K. 2015 Superspreading: mechanisms and molecular design. *Langmuir* **31**, 2304–2309.

VONIOV, O. V. 1976 Hydrodynamics of wetting. *Fluid Dyn.* **11**, 714–721.

WANG, X., CHEN, L., BONACCURSO, E. & VENZMER, J. 2013 Dynamic wetting hydrophobic polymers by aqueous surfactant and superspreader solutions. *Langmuir* **29**, 14855–14864.

ZHU, S., MILLER, W. G., SCRIVEN, L. E. & DAVIS, H. T. 1994 Superspreading of water-silicone surfactant on hydrophobic surfaces. *Colloids Surface* A **90**, 63–78.

https://doi.org/10.1017/jfm.2018.626 Published online by Cambridge University Press